



CHORUS

This is the accepted manuscript made available via CHORUS. The article has been published as:

Exchange bias in epitaxially grown CoO/MgO/Fe/Ag(001)

A. Tan, J. Li, C. A. Jenkins, E. Arenholz, A. Scholl, C. Hwang, and Z. Q. Qiu

Phys. Rev. B **86**, 064406 — Published 3 August 2012

DOI: [10.1103/PhysRevB.86.064406](https://doi.org/10.1103/PhysRevB.86.064406)

Exchange bias in epitaxially grown CoO/MgO/Fe/Ag(001)

A. Tan,¹ J. Li,¹ C.A. Jenkins,² E. Arenholz,² A. Scholl,² C. Hwang,³ and Z. Q. Qiu¹

¹Department of Physics, University of California at Berkeley, Berkeley,
California 94720, USA

²Advanced Light Source, Lawrence Berkeley National Laboratory, Berkeley, California
94720, USA

³Korea Research Institute of Standards and Science, Yuseong, Daejeon 305-340, Republic
of Korea

Abstract

CoO/MgO/Fe/Ag(001) films were grown epitaxially and studied using Magneto-Optic Kerr Effect and X-ray Magnetic Linear Dichroism (XMLD). For thick CoO films we show that both the Fe coercivity and exchange bias exhibit the expected monotonic decrease with increasing MgO thickness. For thin CoO films, however, we find that while the coercivity decreases monotonically, the exchange bias increases initially and then decreases with increasing MgO thickness. By measuring the CoO XMLD as a function of MgO thickness, we show that the unusual behavior of the exchange bias at thinner CoO is due to a transition of the CoO spins from rotatable to frozen spins as the MgO thickness increases.

PACS numbers: 75.70.Ak

1. Introduction

Since the discovery of the exchange bias effect in CoO/Co particles [1], Ferromagnet(FM)/Antiferromagnet (AFM) system has attracted great interest because of its application in spintronics technology [2]. Initial understanding of the exchange bias is that as a FM/AFM system is cooled down within a magnetic field to below the Néel temperature of the AFM layer, the FM/AFM interfacial interaction aligns the AFM interfacial spins to the FM spin direction so that the reversal of the FM spins by an external magnetic field has to overcome the FM/AFM interfacial coupling, leading to an exchange bias field that equals to the interfacial coupling. Although correctly catching the role of the FM/AFM interfacial interaction, this intuitive picture gives an exchange bias several orders of magnitude greater than the experimental values. Two different types of models were proposed to address the above difficulty. The first type assumes a random compensated/uncompensated AFM interface so that the residual interfacial coupling is significantly reduced [3]. The weakness of this model is that the derived exchange bias depends severely on the interfacial roughness and varies from sample to sample which doesn't fully agree with experiment. In addition, this model does not address the FM/AFM interfacial coupling for a perfectly compensated AFM surface. Koon finds that a perfectly compensated AFM surface should couple to a FM layer perpendicularly by canting the AFM spins [4]. However, Schulthess and Butler pointed out that Koon's model should not lead to an exchange bias but only a uniaxial magnetic anisotropy [5]. Different from the first type model that depends heavily on the realistic interfacial roughness and defects, the second type model (referred to as "Mauri's model" [6] based on an earlier model by Néel [28]) considers domain formation near the FM/AFM interface during the FM magnetization reversal. Mauri's model shows that in the strong FM/AFM interfacial coupling limit the exchange bias should correspond to a 180-degree domain wall formation in the AFM layer. While there is experimental evidence of the AFM domain wall formation during the FM magnetization saturation process [7], this model is not valid for ultrathin AFM films that are too thin to host a domain wall. Later development in exchange bias theory is more or less model dependent, aiming to address specific AFM spin configurations or domain structures [8,9,10]. Although Mauri's model does not account directly to ultrathin AFM films, the model does point out an important fact that has been ignored in many theoretical models: one cannot ignore the rotation of the AFM spins in response to the FM magnetization reversal in a FM/AFM system. Recent development in

X-ray Magnetic Linear Dichroism (XMLD) allows a direct measurement of the AFM spins in FM/AFM system. The result shows that there exist rotatable and frozen AFM spins and that these two types of AFM spins play very different roles in the induced exchange bias and magnetic anisotropies [11, 12]. Then taking the interfacial coupling as a phenomenological effective coupling that depends on the interfacial roughness, uncompensated spins, defects, AFM domains, etc., the final exchange bias should be a result of the interplay between the effective interfacial coupling and the AFM frozen spins. To avoid complexity, experimental works usually address the exchange bias by fine-tuning some physical quantities such as the AFM film thickness [13,14] or a spacer layer thickness between the FM and AFM layers. While the former can certainly change the frozen spins in AFM layer [11] and have been widely applied to study exchange bias, the latter could be used to tune the interfacial coupling strength between the FM and AFM layers. For metallic spacer layer, the exchange bias is found to exhibit an oscillatory, non-monotonic, or an exponential decay with the spacer layer thickness [15,16,17,18,19,20]. For insulating spacer layer, the exchange bias has only been reported so far to decay exponentially with the spacer layer thickness [21]. In this paper, we report an experimental study of epitaxially grown CoO/MgO/Fe/Ag(001) single crystalline thin films. We show that as a result of the monotonic decay of the CoO/MgO/Fe interlayer coupling with increasing MgO thickness (d_{MgO}), the exchange bias behave very differently for thin and thick CoO films. For thick CoO films, the exchange bias decays monotonically with increasing the MgO thickness. In the ultrathin limit of the CoO thickness (d_{CoO}), however, the exchange bias increases initially with increasing MgO thickness before resuming the expected monotonic decay. This observation manifests the important role of the CoO frozen spins in generating the exchange bias.

2. Experiment

A Ag(001) single crystal substrate was prepared by mechanical polishing down to a 0.25- μm diamond-paste finish, followed by chemical polishing [22]. The Ag substrate was cleaned in an UHV system by cycles of Ar^+ ion sputtering at $\sim 2\text{keV}$ and annealing at 600°C . A 20-monolayer (ML) Fe film was grown on top of the Ag(001) substrate at room temperature. The film was then annealed at 155°C for about 30 minutes to improve the surface flatness. A MgO wedge (0-4 ML over 3 mm) was then grown on top of the Fe film at room temperature using electron beam evaporation from a MgO target. Then a CoO

wedge (0-25 ML over 3 mm) was grown on top of the MgO wedge by deposition of Co under an oxygen pressure of 2×10^{-6} Torr. The MgO and CoO wedges are orthogonal to each other so that their thicknesses can be varied independently along two orthogonal directions on the sample surface. Fe film on Ag(001) has a bcc structure with the Fe[100] axis parallel to the Ag[110] axis, and CoO film on Fe(001) has a rock salt structure with the CoO[110] axis parallel to the Fe[100] axis [11]. The sample is finally covered by a 2-nm Ag-protection layer. The formation of the Low Energy Electron Diffraction (LEED) confirms the epitaxial growth of single crystalline CoO/MgO/Fe films on Ag(001) substrate (Fig. 1). The sample was measured using Magneto-Optic Kerr Effect (MOKE) and X-ray Magnetic Linear Dichroism (XMLD) at the beamline 4.0.2 of the Advanced Light Source (ALS) of the Lawrence Berkeley National Laboratory. For MOKE measurements, the sample was first cooled down to ~ 90 K from room temperature within a 1000-Oe external magnetic field applied in the Fe in-plane [100] axis. MOKE was used to obtain Fe hysteresis loop of the film. For coercivity greater than 1000 Oe, which is the highest field of our MOKE setup, hysteresis loops were obtained by XMCD measurement at BL 4.0.2 [11]. For measurements at BL 4.0.2, the sample was first cooled down to ~ 80 K from room temperature within a 4000-Oe external magnetic field applied in the Fe in-plane [100] axis.

3. Result and Discussion

We first present the result of CoO/MgO/Fe/Ag(001) for 20ML CoO film ($d_{\text{CoO}} = 20\text{ML}$). At this thickness, all CoO spins are frozen during the Fe magnetization switching. Fig. 2(a) shows representative Fe hysteresis loops at different MgO thicknesses. It is clearly seen that both the coercivity and the exchange bias decrease monotonically with increasing the MgO thickness, showing that the CoO/MgO/Fe interlayer coupling decreases monotonically with increasing the MgO thickness [Fig. 2(b)]. It has been shown that the imaginary wave vector at the Fermi level in insulators gives rise to an exponential decay of the coupling between two ferromagnetic layers across an insulator [23,24]. This was indeed confirmed in experiments [25,26]. Then it is not surprising that the magnetic interlayer coupling in AFM/insulator/FM system should also decay exponentially with the insulating spacer layer thickness [21], though this cannot be true for all thicknesses; for example the non-monotonic dependence for thin CoO. For our sample, the coercivity reached the corresponding bulk Fe value and the exchange bias reached zero at MgO thickness as thin as 4 ML, showing the vanish of the interlayer coupling at 4ML MgO

thickness. The small value of 4 ML MgO thickness indicates a high quality of our epitaxial MgO film on Fe(001) [27], and agrees with the interlayer coupling result in Fe/MgO/Fe sandwiches [26].

We now present the result of CoO/MgO/Fe/Ag(001) at $d_{\text{CoO}} = 5$ ML [Fig. 2(c) and (d)]. Since the interlayer coupling between the CoO and Fe films across the MgO spacer layer should be determined by the MgO thickness; it is easy to understand that the coercivity of this sample also decays monotonically with the MgO thickness, the same behavior as the 20 ML CoO sample. However, as the CoO/MgO/Fe interlayer coupling decreases with increasing the MgO thickness, the exchange bias increases initially to reach a maximum value at ~ 2 ML MgO before the monotonic decay above 3 ML MgO [Fig. 2(d)]. This behavior is unexpected because the exchange bias usually decreases with decreasing the AFM/FM coupling strength.

To ensure the result of Fig. 2, we performed a systematic study on the coercivity and exchange bias as a function of the MgO thickness at different CoO thicknesses (Fig. 3). Regardless of the initial difference at $d_{\text{MgO}} = 0$, the coercivity in CoO/MgO/Fe system [Fig. 3(a)] follows the same trend of the monotonic decay with increasing MgO thickness for all CoO thicknesses. The exchange bias [Fig. 3(b)], on the other hand, exhibits a very different d_{MgO} -dependence at different CoO thicknesses. For thicker CoO ($d_{\text{CoO}} > 15$ ML), the exchange bias behaves similarly to the coercivity, i.e., decreases monotonically with increasing the MgO thickness. For thinner CoO ($d_{\text{CoO}} \leq 15$ ML), the exchange bias initially increases with increasing MgO thickness before resuming the expected monotonic decay at $d_{\text{MgO}} > 3$ ML. The result of Fig. 3 indicates that the coercivity depends mostly on the CoO/MgO/Fe interlayer coupling strength, but the exchange bias depends not only on the interlayer coupling but also something else especially in the thinner limit of CoO.

In an AFM/FM system, the coercivity enhancement does not require frozen spins in the AFM layer but the exchange bias does. This was confirmed by our previous experiment that the CoO/Fe coercivity enhancement occurs at much thinner CoO thickness than the exchange bias [11]. Therefore the result of Fig. 3 shows that the increase of the exchange bias with the MgO thickness in $d_{\text{CoO}} < 15$ ML samples must be associated to the change of the CoO spins (e.g., rotatable/frozen spins) as the MgO thickness increases. As discussed in the introduction, Mauri's model addresses the rotation of the AFM spins near the interface. If the AFM spins are completely frozen due to its anisotropy energy, the FM magnetization reversal will have to overcome the AFM/FM interfacial coupling, leading to

an exchange bias equal to the interfacial coupling. This is the result of the strong anisotropy limit ($\lambda \ll 1$, where λ is the ratio of the interfacial coupling to the AFM domain wall energy) in Mauri's model [6]. In contrast, if the AFM/FM interfacial coupling is much stronger than the AFM anisotropy (for example, infinitely strong interfacial coupling), the FM magnetization reversal will force the AFM spins at the AFM/FM interface to twist and thus creating a 180° domain wall in the AFM layer. Under this condition, the exchange bias corresponds to the domain wall energy in the AFM layer which is the result of Mauri's model in the strong coupling limit ($\lambda \gg 1$) [6]. While Mauri's model correctly points out the importance of the AFM spin rotation in response to the FM magnetization reversal in the strong coupling limit, it cannot be applied to ultrathin AFM film where the AFM film thickness is too thin to host a domain wall formation. In this ultrathin limit, all AFM spins should switch to follow the FM magnetization reversal, leading to a zero exchange bias (or a weak exchange bias if part of AFM spins is still frozen). Noticing that the rotation of the AFM spins is due to the FM/AFM coupling, thus a weakening of the FM/AFM coupling should favor the formation of frozen spins over rotatable spins in the AFM layer. Then the following physical picture can be applied to qualitatively understand our CoO/MgO/Fe/Ag(001) result. For thick CoO films, where the CoO spins are completely frozen at $d_{\text{MgO}} = 0$, the decrease of the CoO/MgO/Fe interlayer coupling by increasing the MgO thickness will certainly keep the CoO spins frozen. The exchange bias under this condition should correspond to the strong anisotropy limit in Mauri's model ($\lambda \ll 1$) so that the exchange bias is determined by the CoO/Fe interlayer coupling across the MgO layer. That is why the exchange bias for $d_{\text{CoO}} > 20$ ML decreases monotonically with increasing the MgO thickness. For thin CoO films, where the CoO spins are totally or partially rotatable at $d_{\text{MgO}} = 0$, the system is in the strong coupling limit in Mauri's model ($\lambda \gg 1$) so that the exchange bias at $d_{\text{MgO}} = 0$ should be zero or very weak for the reason discussed above. As the CoO/Fe interlayer coupling decays monotonically to approach zero with increasing MgO thickness, the CoO/MgO/Fe system should evolve from the strong coupling limit ($\lambda \gg 1$) at $d_{\text{MgO}} = 0$ to the weak coupling limit ($\lambda \ll 1$) at thicker MgO. Consequently, the CoO spins should evolve from rotatable to frozen as the CoO/MgO/Fe interlayer coupling becomes weaker and weaker. Since the exchange bias is zero or very weak in the strong coupling limit ($\lambda \gg 1$) and equals to the AFM/FM coupling in the weak coupling limit ($\lambda \ll 1$), the exchange bias in the CoO/MgO/Fe system in ultrathin CoO limit should increase initially and then decrease as the MgO thickness

increases, which is what we observed for $d_{\text{CoO}} < 15$ ML in Fig. 3.

The above physical picture implies a transition of the CoO spins from rotatable to frozen as the MgO thickness increases for $d_{\text{CoO}} < 15$ ML. To verify this transition, we performed XMLD measurement at $d_{\text{CoO}} = 5$ ML where the CoO spins are totally rotatable at $d_{\text{MgO}} = 0$ within the experimental sensitivity [11]. The CoO L_3 edge absorption spectra are taken for magnetic field parallel and perpendicular to the field cooling direction [Fig. 4(a)]. The difference between these two spectra then measures the amount of rotatable CoO spins. Detailed experimental procedure is described in Ref. 11. Fig. 4(b)-(e) shows two representative spectra at different MgO thicknesses. At $d_{\text{MgO}} = 0.13$ ML, the change of the spectra for field parallel and perpendicular to the field cooling direction corresponds to a complete rotatable CoO spins [11]. At $d_{\text{MgO}} = 3.5$ ML, there is no difference between the spectra for field parallel and perpendicular to the field cooling direction, showing that all the CoO spins are frozen. Using the conventional definition of the XMLD, we retrieve the amount of CoO frozen spins as a function of the MgO thickness in the 5 ML CoO sample. The result shows that the CoO spins becomes frozen gradually as the MgO thickness increases and become completely frozen above 3 ML of MgO [Fig. 5]. We would like to mention that the result of Fig. 5 should be an approximation because it is unclear if the rotatable CoO spins will rotate by 90 degrees or less after the magnetic field rotates by 90 degrees. A reliable theoretical model is needed from the community for the description of exchange bias for partially frozen AFM spins.

We would like to discuss other possible mechanisms that could affect the exchange bias. First, it is shown that the exchange bias in CoO/Fe system is not directly proportional to the CoO frozen spins [11,12]. Instead, there is a “thickness delay” between the exchange bias and the CoO frozen spins. However, the increase of the CoO frozen spins should not decrease the exchange bias provided that other conditions are fixed. In our previous works, the amount of CoO frozen spins is increased by increasing the CoO thickness thus cannot isolate the effect of CoO frozen spins from the CoO thickness. In the present work, the amount of CoO frozen spins is increased without changing the CoO thickness thus providing a cleaner isolation of the CoO frozen spins from its film thickness. On the other hand, because of the lack of a direct proportionality, it is difficult to do a quantitative analysis for Fig. 3(d) in terms of the result of Fig. 5. Second, although the MgO energy gap is stabilized to its bulk value at ~ 3 ML thickness in MgO/Fe(001) [27], the electronic structure of MgO could be varied below 3ML thickness. Then the interesting

question is if the non-monotonic behavior in $H_{\text{ex}}-d_{\text{MgO}}$ could be due to the MgO electronic variation below 3ML especially a possible metallic MgO electronic structure? We think this is unlikely because insulating behavior of MgO was actually observed even at 1ML MgO though the energy gap may be different from its bulk value. In addition we observe a monotonic $H_{\text{ex}}-d_{\text{MgO}}$ relation for thicker CoO film where it is the same MgO film that leads to the non-monotonic $H_{\text{ex}}-d_{\text{MgO}}$ relation at thinner CoO film. Last, it is well known that film and interfacial roughness could affect the exchange bias [28]. Then it is reasonable to ask if the variation of the exchange bias at monolayer regime of MgO thickness could be due to the MgO film roughness and the MgO/CoO interfacial roughness? Note that our sample is CoO/MgO/Fe/Ag(001), there should be the same MgO film roughness and the same MgO/Fe and CoO/MgO interfacial roughness for all CoO thicknesses. Therefore although the film roughness plays a role in determining the absolute exchange bias value, it is unlikely that it is responsible for the different $H_{\text{ex}}-d_{\text{MgO}}$ behaviors at different CoO thicknesses.

4. Summary

In summary, we investigated the exchange bias in epitaxial CoO/MgO/Fe/Ag(001) films. We find that above 20 ML CoO thickness both the Fe coercivity and the exchange bias decreases monotonically with increasing the MgO thickness, showing that the interlayer coupling between CoO and Fe films decreases monotonically with the MgO thickness. Below 17.5 ML CoO thickness, the exchange bias increases initially and then decreases with increasing the MgO thickness. This unusual behavior is explained by a transition of the CoO spins from rotatable to frozen spins as the CoO/Fe interlayer coupling decreases with increasing the MgO thickness. This rotatable-to-frozen transition of the CoO spins with increasing the MgO thickness is confirmed by XMLD measurement.

Acknowledgement

This work was supported by National Science Foundation DMR-1210167, U.S. Department of Energy DE-AC02-05CH11231, and NRF through Global Research Laboratory project of Korea.

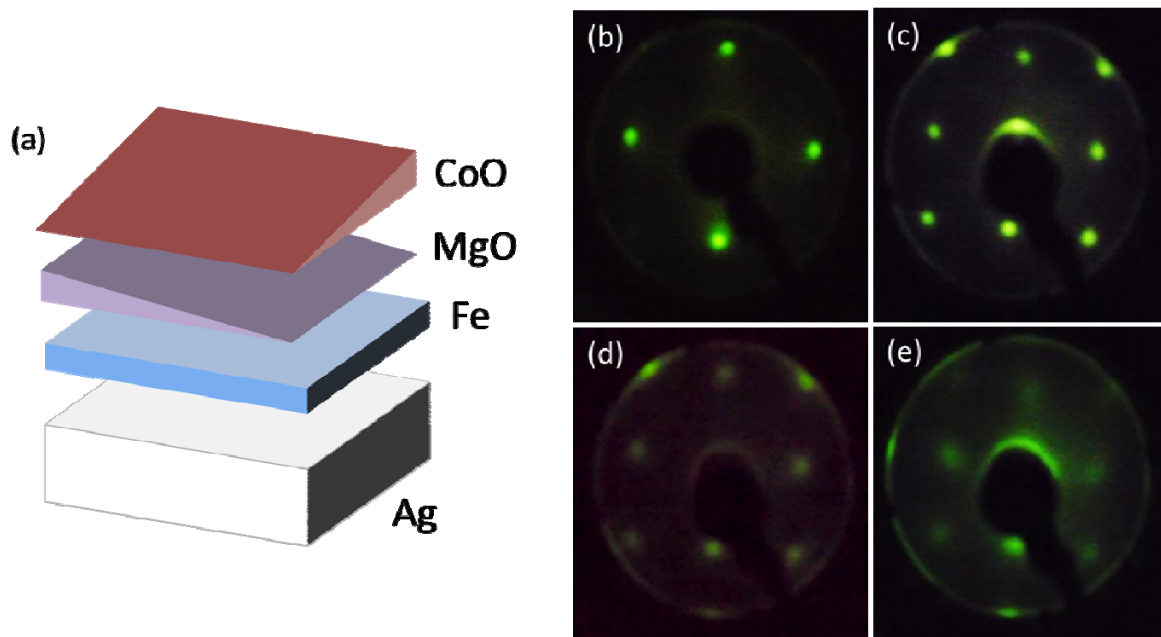


Fig. 1: (color online) (a) schematic drawing of the CoO(0-25 ML)/MgO(0-4 ML)/Fe(20 ML)/Ag(001) double wedged sample. The wedge slope is along the Fe[100] axis. LEED patterns of (b) Ag substrate at 123 eV, (c) Fe layer at 158 eV, (d) MgO layer at 149 eV, and (e) CoO layer at 164 eV. The LEED pattern shows the formation of single crystalline growth of each layer.

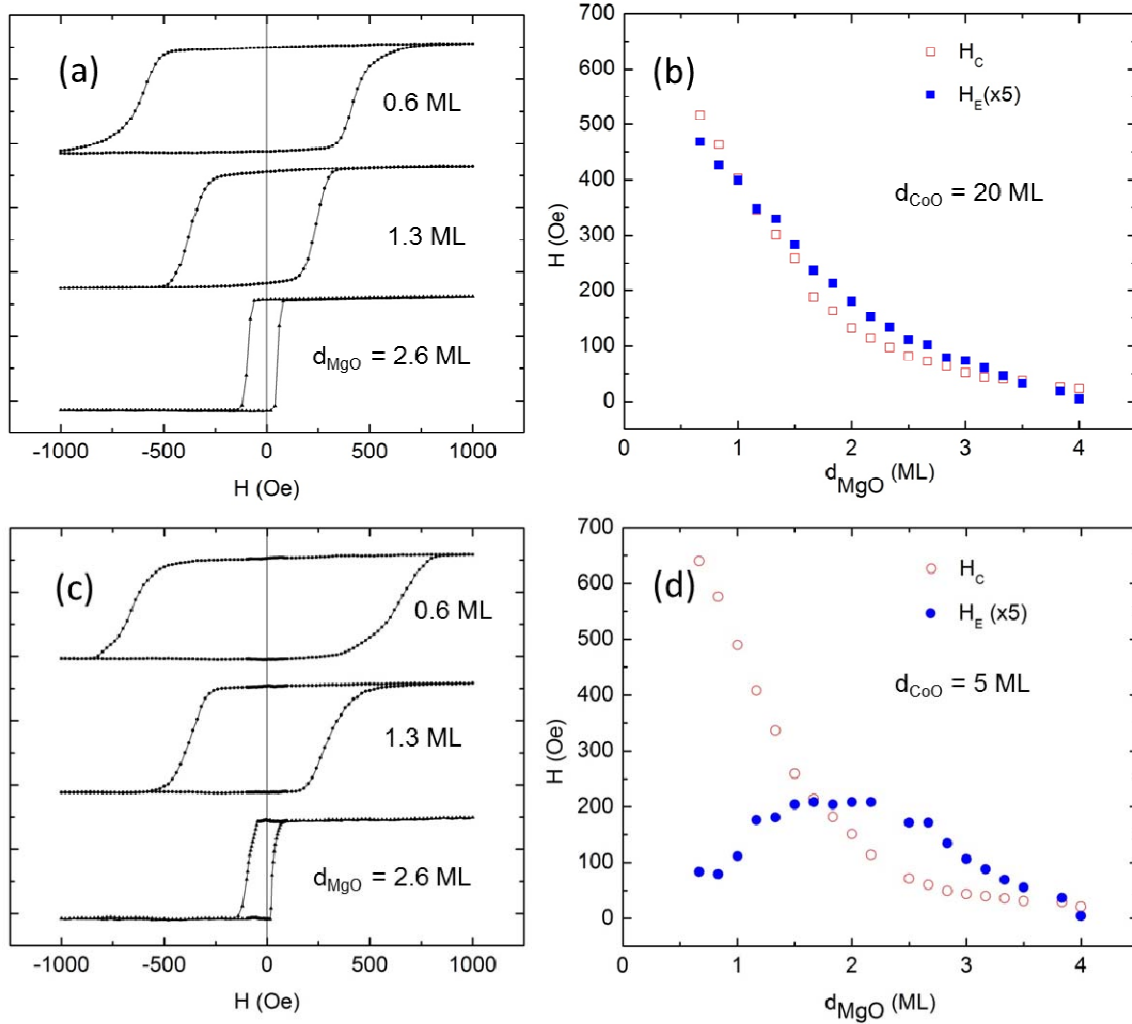


Fig. 2: (color online) (a) Hysteresis loops of CoO(20 ML)/MgO/Fe/Ag(001) at $d_{\text{MgO}} = 0.6$ ML, 1.3 ML, 2.6 ML MgO spacer thicknesses. (b) Coercivity and exchange bias as a function of MgO spacer thickness. Both coercivity and exchange bias decreases monotonically with the MgO thickness, showing that the interlayer coupling across the MgO decreases monotonically with the MgO thickness. (c) Hysteresis loops of CoO(5 ML)/MgO/Fe/Ag(001) at $d_{\text{MgO}} = 0.6$ ML, 1.3 ML, 2.6 ML. (d) Coercivity and exchange bias as a function of the MgO thickness. While the coercivity decreases monotonically, the exchange bias increases initially with increasing the MgO thickness and then decreases at thicker MgO thickness.

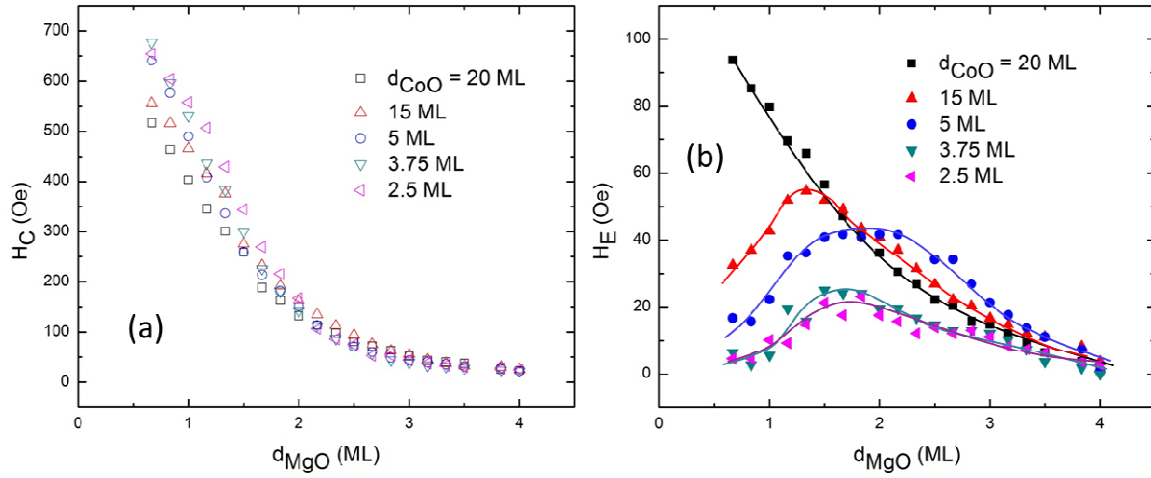


Fig. 3: (color online) (a) Coercivity and (b) exchange bias as a function of MgO thickness at different CoO thicknesses. The coercivity exhibits a monotonic decrease with increasing the MgO thickness for all CoO thicknesses. The exchange bias on the other hand shows an unusual behavior for thin CoO thickness, which is attributed to the rotatable-to-frozen transition of the CoO spins with decreasing the CoO/MgO/Fe interlayer coupling. The solid lines are guide to eyes.

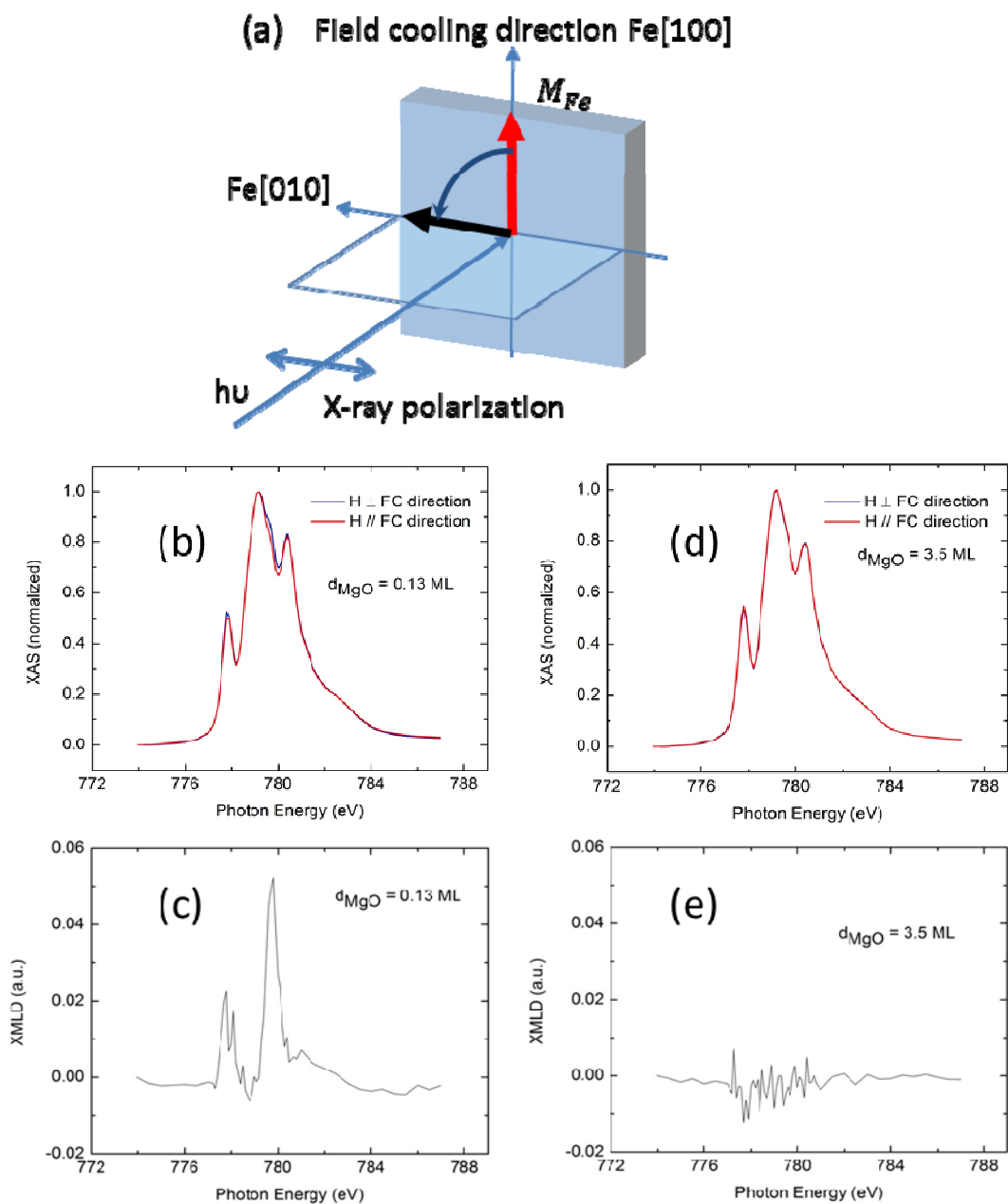


Fig. 4: (color online) (a) XMLD measurement condition. (b) and (d) are the Co L_3 edge X-ray absorption spectra at $d_{\text{MgO}} = 0.13$ ML and 3.5 ML, respectively, for magnetic field applied parallel (red) and perpendicular (black) to the field-cooling direction. (c) and (e) are the differences of the spectra in (b) and (d) respectively, corresponding to the rotatable CoO spins.

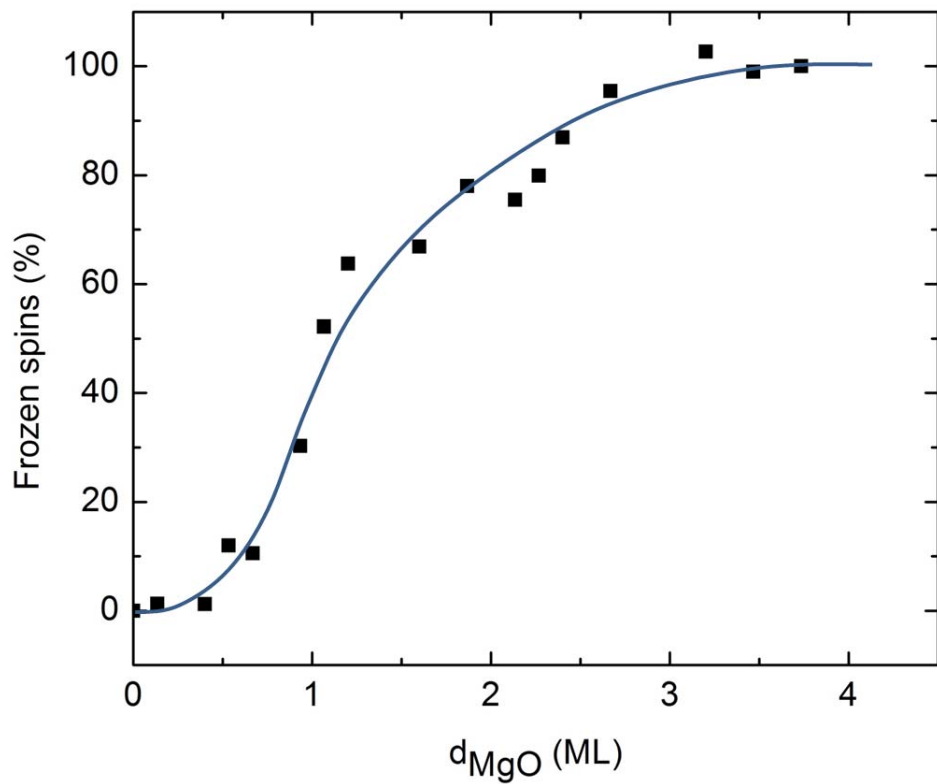


Fig. 5: (color online) Frozen CoO spins in $d_{\text{CoO}} = 5$ ML sample increases as the CoO/MgO/Fe interlayer coupling decreases with the MgO thickness. The solid line is a guide to eyes.

References:

1. W. H. Meiklejohn and C. P. Bean, Phys. Rev. **102**, 1413 (1956).
2. J Nogués and Ivan K. Schuller, J. Magn. Magn. Mater. **192**, 203 (1999).
3. A. P. Malozemoff, Phys. Rev. B **35**, 3679 (1987).
4. N.C. Koon, Phys. Rev. Lett. **78**, 4865 (1997).
5. T. C. Schulthess and W. H. Butler, Phys. Rev. Lett. **81**, 4516 (1998).
6. D. Mauri, H. C. Siegmann, P. S. Bagus, and E. Kay, J. of Appl. Phys. **62**, 3047 (1987).
7. A. Scholl, M. Liberati, E. Arenholz, H. Ohldag, and J. Stöhr, Phys. Rev. Lett. **92**, 247201 (2004).
8. M. D. Stiles and R. D. McMichael, Phys. Rev. B **59**, 3722 (1999).
9. P. Miltényi, M. Gierlings, J. Keller, B. Beschoten, and G. Güntherodt, U. Nowak, and K. D. Usadel, Phys. Rev. Lett. **84**, 4224 (2000).
10. Miguel Kiwi, J. Magn. Magn. Mater. **234**, 584 (2001).
11. J. Wu, J. S. Park, W. Kim, E. Arenholz, M. Liberati, A. Scholl, Y. Z. Wu, Chanyong Hwang, and Z. Q. Qiu, Phys. Rev. Lett. **104**, 217204 (2010).
12. J. Li, Y. Meng, J. S. Park, C.A. Jenkins, E. Arenholz, A. Scholl, A. Tan, H. Son, H. W. Zhao, Chanyong Hwang, Y. Z. Wu, and Z. Q. Qiu, Phys. Rev. B **84**, 094447 (2011).
13. A. L. Kobrinskii and A. M. Goldman, Maria Varela and S. J. Pennycook, Phys. Rev. B **79**, 094405 (2009).
14. Qing-feng Zhan, Wei Zhang, and Kannan M. Krishnan, Phys. Rev. B **83**, 094404 (2011).
15. T. Mewes, B. F. P. Roos, S. O. Demokritov, and B. Hillebrands, J. of Appl. Phys. **87**, 5064 (2000).
16. Luc Thomas, Andrew J. Kellock, and Stuart S. P. Parkin, J. of Appl. Phys. **87**, 5061 (2000).
17. N. J. Gökemeijer, T. Ambrose, and C. L. Chien, Phys. Rev. Lett. **79**, 4270 (1997).
18. M. Gruyters, M. Gierlings, and D. Riegel, Phys. Rev. B **64**, 132401 (2001).
19. V. K. Valev, M. Gruyters, A. Kirilyuk, and Th. Rasing, Phys. Rev. Lett. **96**, 067206 (2006).
20. Y. Meng, J. Li, P.-A. Glans, C. A. Jenkins, E. Arenholz, A. Tan, J. Gibbons, J. S. Park, Chanyong Hwang, H. W. Zhao, and Z. Q. Qiu, Phys. Rev. B **85**, 014425 (2012).
21. S. Nicolodi, A. Harres, L. G. Pereira, J. E. Schmidt, M. A. de Sousa, F. Pelegrini, A. D. C. Viegas, C. Deranlot, F. Petroff, and J. Geshev, J. of Appl. Phys. **110**, 063922

(2011).

22. Nghi Q. Lam, Steven J. Rothman, and L. J. Nowicki, *J. Electro-Chem. Soc.* **119**, 715 (1972).
23. J. C. Slonczewski, *Phys. Rev. B* **39**, 6995 (1989).
24. P. Bruno, *Phys. Rev. B* **54**, 411 (1995).
25. P. A. A. van der Heijden, P. J. H. Bloemen,* and J. M. Metselaar, *Phys. Rev. B* **55**, 11569 (1997).
26. J. Faure-Vincent, C. Tiusan, C. Bellouard, E. Popova, M. Hehn, F. Montaigne, and A. Schuhl, *Phys. Rev. Lett.* **89**, 107206 (2002).
27. Y. Z. Wu, A. K. Schmid, and Z. Q. Qiu, *Phys. Rev. Lett.* **97**, 217205 (2006).
28. L. Néel, *Ann. Phys. (Paris)* **2**, 61 (1967).
28. C. Fleischmann, F. Almeida, J. Demeter, K. Paredis, A. Teichert, R. Steitz, S. Brems, B. Opperdoes, C. Van Haesendonck, A. Vantomme, and K. Temst, *J. of Appl. Phys.* **107**, 113907 (2010).